Ocean Science
Open Access
Discussions

# A new method for continuous measurements of oceanic and atmospheric $N_2O$, CO and $CO_2$: performance of off-axis integrated cavity output spectroscopy (OA-ICOS) coupled to non-dispersive infrared detection (NDIR)

D. L. Arévalo-Martínez[1], M. Beyer[1], M. Krumbholz[1], I. Piller[1,*], A. Kock[1], T. Steinhoff[1], A. Körtzinger[1], and H. W. Bange[1]

[1]Helmholtz Centre for Ocean Research Kiel (GEOMAR), Düsternbrooker Weg 20, 24105 Kiel, Germany
[*]now at: Institute of Physical Chemistry at the Christian-Albrechts-Universität Kiel, Max-Eyth-Str. 2, 24118 Kiel, Germany

---

Title Page

Abstract | Introduction

Conclusions | References

Tables | Figures

◄ | ►

◄ | ►

Back | Close

Full Screen / Esc

Printer-friendly Version

Interactive Discussion

Title Page

Abstract | Introduction

Conclusions | References

Tables | Figures

◄ | ►

◄ | ►

Back | Close

Full Screen / Esc

Printer-friendly Version

Interactive Discussion

**Combined underway measurements of N$_2$O, CO and CO$_2$**

D. L. Arévalo-Martínez et al.

## Abstract

A new system for continuous, highly-resolved oceanic and atmospheric measurements of N$_2$O, CO and CO$_2$ is described. The system is based upon off-axis integrated cavity output spectroscopy (OA-ICOS) and a non-dispersive infrared analyzer (NDIR) both coupled to a Weiss-type equilibrator. Performance of the combined setup was evaluated by testing its precision, accuracy, long-term stability, linearity and response time. Furthermore, the setup was tested during two oceanographic campaigns in the equatorial Atlantic Ocean in order to explore its potential for autonomous deployment onboard voluntary observing ships (VOS). Improved equilibrator response times for N$_2$O (2.5 min) and CO (45 min) were achieved in comparison to response times from similar chamber designs used by previous studies. High stability of the OA-ICOS analyzer was demonstrated by low optimal integration times of 2 and 4 min for N$_2$O and CO respectively, as well as detection limits of $< 40$ ppt and precision better than 0.3 ppb Hz$^{-1/2}$. Results from a direct comparison of the method presented here and well-established discrete methods for oceanic N$_2$O and CO$_2$ measurements showed very good consistency. The favorable agreement between underway atmospheric N$_2$O, CO and CO$_2$ measurements and monthly means at Ascension Island (7.96° S 14.4° W) further suggests a reliable operation of the underway setup in the field. The potential of the system as an improved platform for measurements of trace gases was explored by using continuous N$_2$O and CO$_2$ data to characterize the development of the seasonal equatorial upwelling in the Atlantic Ocean during two *R/V Maria S. Merian* cruises. A similar record of high-resolution CO measurements was simultaneously obtained offering for the first time the possibility of a comprehensive view on the distribution and emissions of these climate relevant gases on the area. The relatively simple underway N$_2$O/CO/CO$_2$ setup is suitable for long-term deployment on board of research and commercial vessels although potential sources of drift such as cavity temperature and further technical improvements towards automation still need to be addressed.

D. L. Arévalo-Martínez
et al.

## 1  Introduction

The assessment of marine emissions of climate relevant gases has become a criti-
cal issue in the attempt to improve our current understanding of the impacts of the
ocean on atmospheric composition and chemistry and therefore, on climate. Atmo-
spheric concentrations of long-lived greenhouse gases such as nitrous oxide ($N_2O$)
and carbon dioxide ($CO_2$) have been increasing at unprecedented rates over the last
century mainly in association with human activities, leading to an overall warming of
the earth's climate system (Denman et al., 2007). Both $N_2O$ and $CO_2$ are strong green-
house gases (Forster et al., 2007), while carbon monoxide (CO) is considered to be an
indirect greenhouse gas that alters the tropospheric photochemistry and enhances the
concentrations of other important reactive gases such as methane and ozone (Bates
et al., 1993; Prather et al., 2001). Despite their importance, vast areas of the ocean
remain uncovered by observational studies of these gases whereas in others tempo-
ral and spatial resolution is coarse due to constrains posed by the sampling intervals
that can be achieved by using discrete and semi-continuous methods, leading to large
uncertainties in marine emissions estimates especially in the cases of $N_2O$ and CO
(Nevison et al., 1995; Stubbins et al., 2006).

In this context, the development and implementation of cost-effective methods for
underway measurements (providing data at frequencies in the order minutes or even
seconds) offers the potential to extend the spatial coverage and temporal resolution
of ship-based observations. The recent development of sensitive analytical techniques
based on infrared detection such as cavity ringdown spectroscopy (CRDS), enhanced
integrated cavity output spectroscopy (ICOS) and off-axis integrated cavity output spec-
troscopy (OA-ICOS) has enabled the detection of a number of trace gases in nanomo-
lar concentrations and opened the possibility to obtain continuous measurements in
a variety of applications including soil and atmospheric monitoring (Baer et al., 2002;
Kasyutich et al., 2003; Maddaloni et al., 2006) as well as in surveys of the surface
ocean (Gülzow et al., 2011; Becker et al., 2012). This represents a great improvement

compared to conventional detection techniques mainly based upon gas chromatography due to the largely increased temporal resolution that can be achieved. Theoretical basis and technical considerations of CRDS, ICOS as well as a comparison with the OA-ICOS approach are presented elsewhere (Mazurenka et al., 2005; Friedrichs, 2008).

Within this set of available techniques, OA-ICOS is particularly interesting due to the high mechanical robustness and relatively simple optical configuration which makes it suitable for long-term measurements in the field. In OA-ICOS a laser beam is injected into an optical cavity in an off-axis alignment such that the multiple modes (transmitted frequencies) produced result in a Lissajous pattern and increased spatial separation between them (Baer et al., 2002; Dyroff, 2011). The spacing between modes in the cavity defines the free spectral range (FSR) which, if kept lower than the laser bandwidth produces enhanced sensitivity. With the above described setup, reflections impacting on each side of the cavity appear as dots forming elliptical patterns which after several rebounds result in a very dense mode spectrum (Herriot et al., 1964; Paul et al., 2001) and consequently a low FSR, thus explaining the improved sensitivity of OA-ICOS based analyzers. Despite the fact that similar sensitivity can be achieved by means of CRDS and ICOS, the associated technical requirements pose difficulties when it comes to obtain data in a high temporal resolution. These constrains seem to be addressed using OA-ICOS because of a comparatively simple configuration and insensitivity to vibration and misalignments (Maddaloni et al., 2006), which highlights the potential advantage of implementing OA-ICOS to perform high-quality at-sea measurements of climate relevant trace gases.

Here, we present for the first time a system capable of performing combined, continuous, high-resolution oceanic and atmospheric measurements of $N_2O$, CO and $CO_2$. This was achieved by coupling an OA-ICOS analyzer and a non-dispersive infrared analyzer (NDIR) to a shower-head (Weiss-type) equilibrator. The combined setup underwent several laboratory tests in order to assess aspects such as precision, accuracy, long-term stability, linearity and response time. Furthermore, it was employed during

**Combined underway measurements of N₂O, CO and CO₂**

D. L. Arévalo-Martínez et al.

Title Page

| Abstract | Introduction |
| Conclusions | References |
| Tables | Figures |

◄◄ ►►

◄ ►

Back Close

Full Screen / Esc

Printer-friendly Version

Interactive Discussion

two oceanographic campaigns in the equatorial Atlantic Ocean to test its performance and to explore its potential for autonomous deployment onboard voluntary observing ships (VOS).

## 2   Instrumentation and methods

### 2.1   Instrumentation

N$_2$O and CO measurements were carried out by a DLT-100 N$_2$O/CO analyzer (Los Gatos Research, Inc., USA) which provides simultaneous measurements of molar fractions of these gases as well as water vapor (H$_2$O) with precision at sub-ppb level. The device is based upon the OA-ICOS technology which combines the use of a high-finesse optical cavity with a continuous wave, narrow-band laser aligned in an off-axis configuration (Fig. 1). A detailed description of the instrument can be found in Baer et al. (2002) and therefore its essential functioning is only briefly described here: an infrared diode laser beam ($\Delta < 1\,\text{MHz}$) is continuously injected into a stainless-steel, cylindrical, 0.28 m long cavity (volume 400 cm$^3$) which is sealed by a pair of highly reflective (99.99 %) mirrors. Since the laser is not oriented at a right angle with respect to the cavity, the number of absorption paths produced is significantly increased resulting in an enhancement of the detected signal (O'Keefe and Deacon, 1988; Maddaloni et al., 2006). The final product is a temporally integrated transmitted light intensity which is then transferred to a digital oscilloscope in interface with a standard internal computer. User interface for data visualization, calibration and other configuration settings consist on a screen on top of the bench and an incorporated keyboard/mouse pad.

During operation, sample air is continuously pumped through the detection cell (cavity) using an internal pump at low flow rates (Lo mode) or an external pump at high flow rates (Hi mode). In the Lo mode the sample gas is directed through an electronic pressure controller placed before the inlet of the cavity, thereby providing isolation from ambient variations in pressure and possible changes in pumping speed. In this study, the

system was set up in the Lo mode with a measured gas flow rate of 235 mL min⁻¹ and a gas pressure of about 106 mbar. Furthermore, all the internal gas connectors were replaced by stainless steel Swagelok® fittings because the original parts were not gas-tight. The cell's temperature and pressure are continually recorded by the instrument and are used as part of the gas molar fraction calculations.

A calibration routine is required during operation in order to ensure accuracy and precision of the measurements. For this, the cavity is flushed with a standard gas mixture of known $N_2O$ and CO concentrations and the system automatically self-calibrates to the input values. As mentioned before, the DLT-100 measures the $H_2O$ molar fraction along with $N_2O$ and CO. This allows the calculation of the dry mole fractions of $N_2O$ and CO, thus accounting for the bias in partial pressure due to the water vapor content of the gas sample (Burch et al., 1962). In order to calculate the dry mole fractions of $N_2O$ and CO, the DLT-100 software performs the following calculation:

$$x(gas)_{dry} = \frac{x(gas)_{wet}}{\left(1 - \frac{xH_2O}{10^6}\right)} \tag{1}$$

where $x(gas)_{dry}$ and $x(gas)_{wet}$ are the molar fractions of the corresponding gas after and before the correction, respectively, and $xH_2O$ is the measured molar fraction of water vapor. Further procedures in order to correct for band broadening effects are possible and have been proven to be stable at different CO concentrations (Zellweger et al., 2012). However, prior drying of the sample gas avoids the need of such corrections and therefore it has been adopted as a customary practice during the measurements (see Sect. 2.3).

For $CO_2$ measurements a NDIR gas analyzer LI-6252 (LI-COR Biosciences, Inc., USA) was used. The instrument is based on the detection of differential infrared radiation (IR) absorption between two cells: one contains the sample of interest (sample cell) whereas the other contains a gas of known $CO_2$ content (reference cell). The reported concentration is proportional to the IR absorption difference among them. Temperature

**Combined underway measurements of N₂O, CO and CO₂**

D. L. Arévalo-Martínez et al.

Title Page

Abstract | Introduction

Conclusions | References

Tables | Figures

|◄ | ►|

◄ | ►

Back | Close

Full Screen / Esc

Printer-friendly Version

Interactive Discussion

D. L. Arévalo-Martínez et al.

and pressure within the cell need to be monitored in order to accurately calculate mole fractions of CO$_2$. The LI-6252 bears a sensor to measure temperature directly in the cell, whereas for pressure measurements an external high-precision ($< 0.05$ %) pressure transducer (SETRACERAM™, model 270) was installed at the outlet of the analyzer such that the analog signal was transmitted to it. The calculations performed by the analyzer's software to determine the CO$_2$ concentrations as well as the internal calibration functions are detailed in the instructions manual (LI-COR, 1996). Small output drifts need to be corrected on a daily basis by adjusting zero and span potentiometers while flushing the cell with synthetic air and the highest standard gas concentration available, respectively. Since the LI-6252 does not include an H$_2$O detection channel, air is dried before being flushed into the cells in order to avoid errors associated with dilution and band broadening effects (McDermitt et al., 1993; Hupp, 2011). Readings were obtained by means of a Matlab$^®$ script running on a standard laptop interfaced to the instrument via serial port. The averaging interval is set to 10 s in order to obtain a low noise level.

## 2.2 Equilibration system

In order to determine the dissolved content of trace gases in seawater, most systems require the analyte to be in gas phase rather than in liquid phase (Johnson, 1999). For this purpose, various designs of equilibrators have been developed and used in conjunction with continuous (Körtzinger et al., 2000) and semi-continuous (Bange et al., 1996b) systems for gas measurements, being particularly suitable since a virtually infinite volume of seawater sample can be directed through the chamber and subsequently analyzed.

A smaller version of the Weiss-type equilibrator (Butler et al., 1988) is used to obtain the equilibrated gas phase to be measured by the N$_2$O/CO and CO$_2$ analyzers. It consists of an acrylic chamber (height: 25 cm, diameter: 15 cm) which is filled with seawater until a headspace of about 3 L is reached. A circular plate with holes is placed on the upper side just beneath the water inlet such that the water dribbles down through

the headspace. The lower part contains the water phase which effectively isolates the headspace into the chamber and is continuously renewed with the ship's water supply system. During operation, the sample air is constantly drawn from the headspace, flows through the analyzers and then returns back to the chamber forming a closed loop. In order to avoid differences with respect to the ambient pressure, the headspace is vented to the atmosphere by means of a Teflon® tube connected to the upper part of the chamber. The estimated error for N$_2$O and CO$_2$ measurements using this type of equilibrator is about 0.2 % or less whereas for CO the error can be as high as 25 % (Johnson, 1999). This difference for CO can be explained by its low solubility and the large gradient between oceanic and atmospheric mixing ratios since it enhances the effect of potential venting of ambient air into the chamber (Conrad et al., 1982; Bates et al., 1995).

## 2.3 Combined setup

A schematic drawing of the underway system is shown Fig. 2. Both analyzers are installed in sequence forming a closed circuit in which equilibrated air circulates through the detectors and flows back to the equilibration chamber with a flow rate of ca. 200 mL min$^{-1}$. Previous tests indicated that no pressure variations are caused on the LI-6252 cell by the action of the internal pump of the DLT-100 and therefore no errors due to pressure differences are expected from the setup itself. Furthermore, both instruments are synchronized to Universal Time Coordinated (UTC) in order to assure temporal comparability of the results, although the measuring interval remains different being 1 s for the DLT-100 and 10 s for the LI-6252. During operation, the water stream is continuously pumped through the equilibrator at a rate of about 2 L min$^{-1}$. In order to avoid interferences associated with the presence of water vapor the air is dried stepwise by conducting it first through a glass cold trap inserted into a 2 L Dewar flask (KWG Isotherm) partially filled with ice and then through a Nafion® tube (model MD-070-72F-4). After drying the sample air flows towards the control unit and ultimately towards

the analyzers before it returns to the equilibrator. A Pall Acro® 50 air filter of pore size 0.2 µm is installed between the drying elements and the control unit in order to prevent water residuals to reach the instruments. Teflon® (PTFE) tubing is used to draw all the connections between the equilibrator and the control unit and to the analyzers.

5 The equilibration temperature is measured by placing an EASYLOG 40KH temperature logger (±0.01 °C) inside the equilibrator, while the equilibration pressure is assumed to be very close to atmospheric pressure since the headspace is permanently vented to ambient air. Pressure readings are taken from the ship's data distribution system.

The control unit contains all the stainless steel valves (Swagelok®) used to regulate
10 the air flow through the gas lines switching between equilibrator, ambient and standard gases. These valves are operated manually and have different configurations of opening/closing depending on the gas being measured. It's worth noting however, that no matter which combination is used there must be always air flowing towards the analyzers because the DLT-100 is sensitive to strong pressure differences that may arise
15 from the total closure of the gas line. A 3-way valve is used to separate the equilibrator gas circuit from the atmospheric air/standard gases circuit (Fig. 2).

Ambient air is pumped at a rate of $350\,mL\,min^{-1}$ using an Air Cadet™ pump (Thermo Scientific), dried using the same approach as for the gas stream from the equilibrator and then conducted through the gas analyzers. In this case, a control valve is switched
20 to prevent air from the equilibrator to pass through the Nafion® tube. In field applications the great distance between the air intake and the location of the system might create difficulties for a proper flushing of the lines. Therefore, during ambient air measurements the pump is always switched on approximately 5 min before the measurements to ensure a complete flushing of the intake gas lines. In contrast to the headspace air,
25 ambient air is discarded via a 3-way valve which is configured to direct the flow to a 2 m long plastic hose which is open to the laboratory air.

In order to account for possible drifts of the system (DLT-100) and to calibrate final data (LI-6252), control measurements of standard gas mixtures of $N_2O$, CO and $CO_2$ in synthetic air as well as compressed air are performed at regular intervals. The

standard gases used (Std.1: 362.3 ppb $N_2O$, 233.5 ppb CO, 200.0 ppm $CO_2$; Std.2: 746.0 ppb $N_2O$, 255.5 ppb CO, 602.0 ppm $CO_2$) were prepared by Deuste-Steiniger GmbH (Mühlhausen, Germany) and calibrated at the Max Planck Institute for Biogeochemistry (Jena, Germany) against the National Oceanic and Atmospheric Administration (NOAA) standard scale. The exhaust gas from the control measurements is also discarded like the ambient air by switching the 3-way valve to "waste" position.

During field deployment, ambient air and control measurements are conducted every six hours over a period of approximately 5 min for each gas. Zero and span adjustments for the LI-6252 are conducted every 24 h by using synthetic air and the standard 2 whereas the DLT-100 calibration is made every two weeks. As a result, each 6 h period of seawater measurements is bracketed by control measurements of standard gases, thus allowing further correction procedures of the raw data before final computations are made.

## 3 Assessment of system performance

### 3.1 Response time of the equilibrator

A given gas phase in equilibrium with the underlying water phase in the equilibrator chamber is assumed to adjust to changing water properties within a time frame given by the response time for the gas of interest. This re-equilibration process is mainly dependent on factors such as the type of chamber, water flow and the solubility of the different gases (Johnson, 1999). The time constant of the equilibrator $\tau$, defined here as the time interval needed for a given concentration difference between water and gas phases to decrease exponentially to 1/e of the initial value, was determined experimentally and is used as an indicator of the chamber's performance. For this, a step experiment was carried out by using two reservoirs of water with different $N_2O$ concentrations. In order to produce distinct $N_2O$ levels two 100 L tanks were filled with freshwater and whereas one of them was led exposed to ambient (laboratory) air ($N_2O = 402.4$ ppb)

the other was manipulated by aeration with a standard gas for approximately 3 h until a $N_2O$ molar fraction of 570 ppb was reached. The water from the tanks was supplied to the equilibrator by means of a 3-way valve, thus allowing a rapid switching between reservoirs. Moreover, a control valve was installed before the equilibrator's inlet to sus-
5  tain a water flow of about 2 L min$^{-1}$.

Water from both reservoirs was successively conducted though the equilibrator until steady readings were achieved (SD < 0.2 ppb). Once stable readings were obtained for the enhanced concentration reservoir the flow was switched to the second reservoir with lower concentration and the change was continuously recorded. Assuming that
10  the re-equilibration of the headspace gas follows first order kinetics, the process can be described by the following equation:

$$\frac{dp_g}{dt} = k\left(p_w - p_g\right) \tag{2}$$

where $p_g$ and $p_w$ are the $N_2O$ concentrations in the gas and water phases, respectively, and $k$ is equivalent to $\tau$, an indicator of how fast the equilibrator responds to changes
15  in the gas concentration of the water phase. Integration of Eq. (2) yields the following exponential equation:

$$p_g = p_w + \left(p_g^0 - p_w\right)e^{-\tau t} \tag{3}$$

with $p_g^0$ and $p_w$ being the $N_2O$ concentrations of the enhanced and ambient air reservoirs, respectively, and $p_g$ the recorded gas concentration at a given time $t$. The time
20  constant $\tau$ can be calculated from the slope of the change in $N_2O$ concentration over time after arranging Eq. (3). A plot of $-\ln(p_g - p_w/p_g^0 - p_w)$ vs. time shows a strong linear correlation, justifying the assumption of first order kinetics for the equilibration process (Fig. 3). The step experiment was repeated several times and resulted in a value for $\tau$ of $145 \pm 20$ s (approx. 2.5 min). A much longer $\tau$ was found for CO during the same
25  experiment, indicating that the equilibration process for this gas takes ca. 45 min. Such

Title Page

Abstract | Introduction

Conclusions | References

Tables | Figures

◄ | ►

◄ | ►

Back | Close

Full Screen / Esc

Printer-friendly Version

Interactive Discussion

difference is expected due to the low solubility of CO in seawater (Wiesenburg and Guinasso, 1979) and it has been observed before for a similar equilibrator by Johnson (1999). The values predicted from that study are much larger (6.4 min $N_2O$ and 216.3 min CO), which might be due to the different size of the equilibration chamber.

5  Since the equilibrator in our system is comparatively small, the volume of headspace gas that needs to be equilibrated with the water stream is lower thus enhancing the speed with which the process takes place.

Due to the similar solubilities of $N_2O$ and $CO_2$ (Weiss, 1974; Wilhelm et al., 1977; Weiss and Price, 1980) we assume that the time constant for both gases is also com-

10  parable under the same setup. This result lies within the range of observations from step experiments carried out at different $CO_2$ concentrations in equilibrators of distinct designs, with time constants which vary between 0.76 min and 3.76 min (Körtzinger et al., 1996; Gülzow et al., 2011). Likewise, the obtained values for $\tau$ were in the same range as those reported by Butler et al. (1988) and Weiss et al. (1992) for a similar

15  Weiss equilibrator. Thus it can be stated that the equilibrator performs well, responding fast enough to achieve measurements of gases like $N_2O$ and $CO_2$ on minute scale temporal resolution. On the other hand, such fine resolution for CO measurements is constrained by its low solubility because it delays the equilibrium process. However, in this case the major oceanic sources (microbial and photochemical production) and

20  sinks (microbial consumption and air-sea gas exchange) of CO alter its concentrations over periods of several hours (Kitidis et al., 2011) and therefore the features of diurnal variability can still be detected by the DLT-100 when is coupled to the equilibrator. Further improvement of the temporal resolution for CO measurements with this method could be achieved by enhancing the equilibration process with equilibration chambers

25  that bear a higher exchange surface and increased water flow.

## 3.2 Precision and accuracy

The quality of any system for high-sensitivity measurements is largely determined by its stability because it dictates for how long the produced signal can be averaged be-

**Combined underway measurements of $N_2O$, CO and $CO_2$**

D. L. Arévalo-Martínez et al.

Title Page

| Abstract | Introduction |
| Conclusions | References |
| Tables | Figures |

Back | Close

Full Screen / Esc

Printer-friendly Version

Interactive Discussion

fore drift effects influence the data. Here, the concept of Allan variance ($\sigma_A^2$) is used to characterize the system's stability and short-term precision (Allan, 1966). For a given set of adjacent measurements $\sigma_A^2$ tends to decrease with increasing integration times as long as random noise dominates over instrumental drift. When higher integration times are considered, however, drift tends to increase and $\sigma_A^2$ starts to rise indicating a reduced performance of the system. This means that during the time phase dominated by random noise, $\sigma_A^2$ is equivalent to the statistical variance of the measurements and therefore its square root provides an estimation of the detection limit (Werle et al., 1993; Kroon et al., 2007). Since the LI-6252 and similar models are well-established instruments that have been extensively tested as part of autonomous systems for $CO_2$ measurements (Pierrot et al., 2009) the analysis here is centered on the DLT-100 analyzer.

Continuous measurements of a gas with molar fractions of $362.73 \pm 0.59$ ppb $N_2O$ and $233.32 \pm 0.46$ ppb CO (mean $\pm$SD) over a period of 15 min and a sampling rate of 1 Hz were used to calculate $\sigma_A^2$. Subsequently $\sigma_A^2$ was plotted against the integration time and as can be seen in Fig. 4 minimum $\sigma_A^2$ was attained at integration times of 120 s and 240 s for $N_2O$ and CO, respectively. These values correspond to the optimal integration times for the analyzer. Even though at higher integration times drift tends to increase, the DLT-100 has been found to be stable within $\pm 0.6$ ppb $N_2O$ and $\pm 0.4$ ppb CO over a time period of 5 h (not shown). Similar optimal integration times (2–5 min) were obtained for CO with an OA-ICOS based analyzer by Zellweger et al. (2012), with values being stable within $\pm 0.1$ ppb over a 10 h period.

By making use of the Allan standard deviation ($\sigma_A$), i.e. the square root of the minimum $\sigma_A^2$, the detection limit of the system can be estimated (Werle et al., 1993). Thus, for $\sigma_A^2 = 1.4 \times 10^{-3}$ ppb$^2$ $N_2O$ and $\sigma_A^2 = 5.9 \times 10^{-4}$ ppb$^2$ CO the corresponding detection limits of the DLT-100 are 37 ppt for $N_2O$ and 24 ppt for CO. Detection limits in the order of 50 and 60 ppt have been reported for $N_2O$ measurements using quantum cascade laser (QCL) spectrometers (Nelson et al., 2004; Kroon et al., 2007). On the other hand, our values are higher than the 10 ppt detection limit reported by Zellweger

Title Page

Abstract | Introduction

Conclusions | References

Tables | Figures

◄ | ►

◄ | ►

Back | Close

Full Screen / Esc

Printer-friendly Version

Interactive Discussion

et al. (2012) for CO measurements with the same type of OA-ICOS analyzer. Nevertheless, the obtained results still satisfy the high standard requirements proposed for instruments used in sensitive measurements of trace gases (Nelson et al., 2004) and feature improved detection limits compared to QCL instruments.

Nelson et al. (2004) suggested a value of 1 ppt of the ambient mixing ratio as the optimal precision to be achieved for highly-sensitive field measurements of $N_2O$. With an ambient mixing ratio of 320 ppb, this is equivalent to a precision of $0.3\,\mathrm{ppb\,Hz}^{-1/2}$. An estimate of the short-term precision of the DLT-100 was obtained by means of the expression:

$$\sigma = \sigma_A \cdot f_s^{-1/2} \tag{4}$$

where $\sigma_A$ is the Allan standard deviation in ppb and $f_s$ is the sampling frequency in Hz. Precisions of $3.8 \times 10^{-2}\,\mathrm{ppb\,Hz}^{-1/2}$ for $N_2O$ and $2.4 \times 10^{-2}\,\mathrm{ppb\,Hz}^{-1/2}$ for CO were achieved. These values are comparable to those reported for other OA-ICOS analyzers using the same measurement rate (Hendriks et al., 2008; Zellweger et al., 2012), and are lower compared to those obtained by Kroon et al. (2007) for a QCL analyzer operated at 10 Hz ($0.5\,\mathrm{ppb\,Hz}^{-1/2}$). The results also evidence an improvement in the precision achieved for $N_2O$ and CO measurements by employing OA-ICOS in comparison with the use of gas chromatographic methods (Weiss, 1981; Bates et al., 1995; Bange et al., 1996a). Altogether the stability and high precision of the DLT-100 analyzer, capable of detecting concentration changes in the sub-ppb range, makes it suitable not only for continuous long-term monitoring of $N_2O$ and CO but also for detailed surveys of fine structure features of their distribution and fluxes.

## 3.3 Long-term stability of the calibration

Continuous deployment of the DLT-100 in the field supposes the need of low maintenance and also requires the instrument to deliver stable results for extended periods of time. In order to test the instrument's stability after calibration, standard gases with

different molar fractions were measured at fixed intervals (5 min) for 14 days. At the be-
ginning, the analyzer was calibrated by using a reference gas containing 362.3 ppb N$_2$O
and 233.5 ppb CO and subsequently the gases were supplied in increasing concentra-
tion order at 5 instances. A 3 min average was calculated for each gas (SD < 0.2 ppb)
and the results were used to quantify the offset of the measurements with respect to
the standard values by using:

$$\text{MD} = \frac{M - S}{S} \tag{5}$$

where $M$ and $S$ are the measured and standard gas values in ppb, respectively. No
significant drift for N$_2$O was observed during the 2 weeks, with highest deviations being
lower than 0.2 % and a maximum of 1 % due to occasional concentration changes in
the order of 2 ppb (Table 1). For CO the deviations were somewhat higher mainly due to
uncertainties on the concentration of the reference gases. Nevertheless, the observed
drift for CO remained within less than 2 % during the first week and increasing only
on the last days due to mole fraction differences in the order of 3–4 ppb. Furthermore,
a two point calibration factor was computed for each measurement period by means
of:

$$F_{\text{cal}} = \frac{S_H - S_L}{M_H - M_L} \tag{6}$$

with $S_H$ and $S_L$ being the highest (746.0 ppb N$_2$O) and lowest (322.5 ppb N$_2$O) standard
values, respectively, and $M_H$ and $M_L$ being the corresponding high and low measured
values (3 min average). Such factor was calculated only for N$_2$O since the concentra-
tion difference between CO standards was only 20 ppb. A mean value of 1.01 for $F_{\text{cal}}$
with variations smaller than 0.1 % during the measurement period evidenced the high
accuracy of the DLT-100. Based on these results it can be stated that, upon calibra-
tion, the instrument provides N$_2$O and CO measurements without significant drift for
a period of at least 2 weeks. Accuracy in N$_2$O measurements was slightly lower for

the high concentration standard (746.0 ppb) during the experiment mainly due to the fact that the values are further apart from the single calibration point of the instrument. Such effect does not impair the DLT-100 general performance and the measurements are highly accurate, although at even higher concentration ranges a more frequent calibration might be necessary.

## 3.4 Linearity

The linearity of the DLT-100 was assessed by preparing dilutions of standard gases in synthetic air and measuring them sequentially for 10–15 min periods. The desired dilutions were achieved by means of two mass flow controllers (red-y smart series, Vögtlin Instruments AG, accuracy ±0.3 %) connected to the analyzer while in interface with the commercially available software EasyHTK (HTK Hamburg GmbH, Germany) that produced gas mixtures with the targeted concentrations. Two sets of dilutions were done so as to cover the upper and lower boundaries of the operational range of the instrument, in which its response is expected to be linear. The first set of dilutions encompassed the range between 0 to 750 ppb $N_2O$ and a quadratic function was found to better fit the response of the DLT-100 within that concentration interval (top panel, Fig. 5). It is worth nothing however, that the regression residuals showed only slight departures from linearity and therefore the quadratic term only improves the residuals by $< 0.001$ % (linear fit: $y = 0.99x + 1.47$, $r^2 = 0.9998$). Thus, in practical terms the analyzer might be as well regarded as linear for $N_2O$. Recently, Zellweger et al. (2012) performed a similar test on the same type of analyzer and found also a quadratic function to be more appropriate to characterize the instrument response during CO measurements (regression residuals within ±0.2 ppb).

The second set of dilutions was prepared in the range between 2800 and 4000 ppb in order to assess the response of the DLT-100 when exposed to high levels of $N_2O$ and CO like those found in places of strong outgassing to the atmosphere (Bange et al., 1996b; Kitidis et al., 2011). Figure 5 (bottom panel) shows the results of this test, wherein the DLT-100 performance is also best characterized by a quadratic fit for both

**Combined underway measurements of $N_2O$, CO and $CO_2$**

D. L. Arévalo-Martínez et al.

Title Page

Abstract | Introduction

Conclusions | References

Tables | Figures

◄ | ►|

◄ | ►

Back | Close

Full Screen / Esc

Printer-friendly Version

Interactive Discussion

N$_2$O and CO. Like in the lower concentration range, the linear approach also represents well the response of the analyzer for both gases (linear fits: N$_2$O $y = 1.02x + 87.57$, $r^2 = 0.9999$; CO $y = 0.94x + 61.43$, $r^2 = 0.9999$). Thus it can be inferred from these observations that the response of the DLT-100 is rather uniform in both the lower and upper boundaries of its operational range for N$_2$O and CO, and that it can be best represented by quadratic functions.

## 4 At-sea tests

The underway system was deployed during two oceanographic campaigns to the equatorial Atlantic Ocean on board of the R/V *Maria S. Merian* (MSM 18 legs 2 and 3, Fig. 6). Seawater was taken from the ship's water supply system (centrifugal pump) which draws water from two inlets at the bottom of the vessel at approximate 6 m depth, and it was continuously pumped through the equilibrator at a rate of 2 L min$^{-1}$. Atmospheric measurements were accomplished by pumping ambient air from the ship's mast at approximately 30 m height and leading it to the system by means of polyethylene/aluminum tubing (Synflex$^®$ 1300) at a rate of 350 mL min$^{-1}$. A detailed description of the measurement setup is given in Sect. 2.3.

As depicted in Fig. 7, standard gas measurements made every 6 h over a period of 64 days evidenced only slight drifts of the DLT-100 for N$_2$O (mean offset = 0.005 ppb). Most measurements fluctuated within 1 % of the standard value (362.3 ppb N$_2$O) with a maximum of 1.4 % and no discernible trend of increase or decrease was found over time spanned by the two cruises. Similar results were obtained for CO during MSM 18-2 with stable values within ±1 % of the reference gas (233.5 ppb CO). In the course of MSM 18-3 however, high scatter was observed with deviations as high as 5 % (10 ppb CO) indicating a strong decrease in accuracy. Given that the DLT-100 did not exhibit such problem during laboratory tests carried out after the cruises, it is unlikely that this bias was the result of malfunctioning of the laser or presence of particles on the cavity. Instead, marked changes in ambient temperature could have driven the steep

changes in the detected signal of CO during MSM 18-3. From the time series of CO and temperature data recorded by the DLT-100 during both cruises it can be seen that indeed the strong temperature changes after 1 July coincide with elevated (though highly variable) CO values for the standard gas during MSM 18-3. Analysis of N$_2$O and temperature data for the same period indicated that the effect is considerably lower for N$_2$O with maximum drift values of ca. 3 ppb for the same temperature change (6 $^\circ$C). In contrast to this results, Zellweger et al. (2012) found only slight deviations on standard gas measurements of CO ($-0.4 \pm 1.1$ ppb) while using the same type of analyzer during temperature manipulations under controlled conditions. Although the simulated temperature changes during their tests were on the same order of magnitude of the observed changes during MSM 18-3, they spanned a much lower range of temperatures than our field observations (32–38 $^\circ$C) and therefore may not be directly comparable. Overall, these results suggest that although the analyzer is stable over long time periods, care must be taken to ensure proper ventilation and that corrections are developed to account for the effects of temperatures close to the upper boundary of the analyzer's recommended operating temperature (35 $^\circ$C).

The performance of the N$_2$O/CO/CO$_2$ system in the field was evaluated by comparison with well-established methods. Since no discrete method for CO measurements was available during the cruises, the assessment was done based on N$_2$O and CO$_2$ data and only underway CO data are presented. Discrete samples were taken on a daily basis from a bypass connected to the same water source that supplied the underway system. For N$_2$O, triplicate samples were collected in 20 mL brown glass flasks which were rinsed twice their volume before filling; rubber butyl septa were used to seal the flasks after collection and each sample was visually inspected to confirm absence of air bubbles. Metallic caps were crimped to each flask so as to avoid air exchange between the sample and the ambient air. A headspace was created on each sample by replacing 10 mL of water with synthetic air (99.999 %, AirLiquide, Düsseldorf, Germany). Subsequently, samples were stirred using a Vortex-Genie$^\circledR$ 2 mixer (Scientific Industries Inc., USA) and poisoned with 0.5 mL of HgCl$_2$. Samples were stored at room

temperature and after an equilibration time of at least 2 h were analyzed using a GC-ECD system (Hewlett Packard (HP) 5890 Series II gas chromatograph equipped with a HP 19233 ECD (Agilent Technologies, Santa Clara, CA, USA)). The separation procedure was carried out in a stainless steel column (long: 1.83 m, external diameter: 3.2 mm, internal diameter: 2.2 mm) with a molecular sieve of 5 Å (W.R. Grace & Co. Conn., Columbia, USA). At least four standard gas mixtures up to 933 ppb $N_2O$ were used to establish calibration curves for the measurements in order to estimate the $N_2O$ concentration from the integrated peak areas of the chromatograms. The concentration of dissolved $N_2O$ was calculated using the expression by Walter et al. (2006). Final absorption data from the DLT-100 is reported in terms of dry molar fraction of the corresponding gas. Thus the concentration of $N_2O$ in seawater was calculated using the expression by Weiss and Price (1980):

$$C_{N_2O} = \beta \cdot x' \cdot P \tag{7}$$

where $\beta$ is the Bunsen solubility (in $mol\,L^{-1}\,atm^{-1}$) computed with the equation of Weiss and Price (1980) at equilibration temperature and in situ salinity, $x'$ is the measured dry molar fraction of $N_2O$ and $P$ the ambient pressure. Differences between in situ and equilibration temperature were taken into account by applying the correction from Walter et al. (2004):

$$C_{N_2O_{sw}} = C_{N_2O} \cdot \left( \frac{\beta_{EQ}}{\beta_{SST}} \right) \tag{8}$$

where $\beta_{EQ}$ and $\beta_{SST}$ are the Bunsen solubilities at equilibration and in situ temperature, respectively.

Samples for $DIC/T_A$ determinations were collected in 500 mL, borosilicate glass bottles (Schott Duran®) with ground glass stoppers and were treated according to the procedures described in Dickson et al. (2007). DIC was measured by means of the coulometric method using a Single Operator Multi-parameter Metabolic Analyzer (SOMMA)

1300

(Johnson et al., 1993) whereas $T_A$ was measured by potentiometric titration as described by Mintrop et al. (2000). Seawater $CO_2$ fugacity ($fCO_2$) was computed using a MS-Excel macro written by Dr. D. Pierrot (AOML-NOAA), which is based upon the code originally developed by Lewis and Wallace (1998). In the parameterization used seawater pH scale (mol kg – sw$^{-1}$) was chosen and the dissociation constants for carbonic acid ($K_1$, $K_2$) from Mojica-Prieto and Millero (2002) were employed. The dry molar fractions of $CO_2$ delivered by the LI-6252 were calibrated and used to compute in situ $fCO_2$ according to the recommended procedures described in Dickson et al. (2007).

Concentrations of dissolved CO were computed by means of a similar expression as in Eq. (7) but adding a correction for water vapor effects and the Oswald solubility coefficient $\alpha$. Thus, CO molar concentrations were obtained from the product of the gas partial pressure and its solubility at equilibration temperature and in situ salinity (Bates et al., 1995):

$$C_{CO} = \left[ x' \cdot P_a - P_w \right] \cdot \alpha \tag{9}$$

where $x'$ is the measured gas molar fraction, $P_a$ is the atmospheric pressure, $P_w$ is the saturation water vapor pressure at equilibration temperature and salinity (Weiss and Price, 1980) and $\alpha = \beta \cdot (T_K/273.15)$ with $\beta$ being the Bunsen solubility of CO (Wiesenburg and Guinasso, 1979) and $T_K$ the absolute temperature in the equilibrator (in K). A correction in order to account for temperature differences between the water intake and the equilibrator was performed by using the ratio of the solubilities ($\alpha$) at equilibration and in situ temperatures. All values are expressed in nmol L$^{-1}$ after dividing $C_{CO}$ by the molar volume of CO at standard pressure and temperature (Stubbins et al., 2006). The saturation ratios were obtained after dividing $C_{CO}$ by the expected concentration of dissolved CO while in equilibrium with the atmosphere (Stubbins et al., 2006). Light measurements (Photosynthetically Active Radiation, PAR) were carried out along the cruise track by using a Messen-Nord radiation measurement system (SMS-1 A) installed at the vessels antenna.

Full Screen / Esc

Printer-friendly Version

Interactive Discussion

**Combined underway measurements of N$_2$O, CO and CO$_2$**

D. L. Arévalo-Martínez et al.

Plots of discrete vs. underway $C_{N_2O}$ and $f$CO$_2$ show a rather good agreement between both methods (Fig. 8) and the strongest deviations occurred during the crossing through sharp gradients. This can be explained by the fact that continuously recorded data resolves much better features which might be otherwise interpreted as noise.

Aside of these differences, the proximity between the results obtained by both methods indicates a good performance of the underway system. An additional evaluation of the performance of the LI-6252 used as part of this study was carried out by running a separate underway system for CO$_2$ measurements from General Oceanics, Inc., USA (hereafter called GO). GO was operated in parallel to the N$_2$O/CO/CO$_2$ system using the same water source as well as the same standard mixtures of gases. A detailed description of the GO system can be found in Pierrot et al. (2009). Despite some differences in the general design and the fact that the GO system runs autonomously, the principle of measurement is the same: sample air is drawn from an equilibration chamber, detected using a NDIR gas analyzer (model LI-6262) and returned back to the chamber forming a closed circuit. After MSM 18-2 a large leakage was detected at the internal components of the NDIR analyzer of the GO and therefore only data from MSM 18-3 were used for the comparison. Figure 9 shows the spatial distribution of $f$CO$_2$ values computed from data collected by the N$_2$O/CO/CO$_2$ system described here and the GO for a cruise track between 15° N and 5° S. It can be seen that both data sets are consistent to within ±1.6 µatm over the whole cruise. $f$CO$_2$ from the sensor at the N$_2$O/CO/CO$_2$ system is somewhat higher than $f$CO$_2$ from GO, but nevertheless both systems agree to within the recommended target of 2 µatm for high-quality oceanic CO$_2$ measurements (Pierrot et al., 2009). In line with these observations, the results of a regression analysis also indicated a reliable operation of the N$_2$O/CO/CO$_2$ underway system when results are compared to those delivered by GO ($y = 1.00x -$ 1.67, $r^2 = 0.995$, $n = 16522$).

Measurements of atmospheric gas mixing ratios of N$_2$O, CO and CO$_2$ were in reasonably good agreement with monthly mean mixing ratios from the NOAA ESRL Carbon Cycle Cooperative Global Air Sampling Network station at Ascension Island

(hereafter ASC, 7.96° S 14.4° W, http://www.esrl.noaa.gov/gmd/dv/site/site.php?code=ASC). A summary of the results is presented in Table 2. $N_2O$ values varied between 320.41 and 326.12 ppb with an average monthly mean of $323.04 \pm 0.96$ ppb. This value is somewhat lower than the mixing ratio reported for May–July at ASC ($324.09 \pm 0.40$ ppb; Dlugokencky et al., 2011) but the temporal and spatial trends were well represented with no major changes after two months of measurements and no significant latitudinal gradient. This suggests a rather uniform distribution of atmospheric $N_2O$ over the equatorial Atlantic, which is expected due to the lack of relevant sources or sinks of this gas in the troposphere (Prather et al., 2001).

In contrast, CO gas mixing ratios were highly variable fluctuating between 51.16 and 153.99 ppb (mean $92.92 \pm 18.19$ ppb) with a slight increase over time (maximum values were observed in mid-July). These results are comparable with the range of observations obtained at ASC between May and July 2011 (58.04–123.77 ppb) and also depict part of the seasonal cycle of atmospheric CO in the area, which is characterized by a sharp increase from ca. 60 ppb in May to about 120 ppb in July when the maximum values of the annual cycle are reached (Novelli and Masarie, 2012). The CO monthly mean at ASC differs considerably with respect to our measurements ($83.20 \pm 16.60$ ppb) although is in the same range of uncertainty. Such dissimilarities are likely due to spatiotemporal variability which is not equally represented in the two data sets; this affects the comparison strongly because of the inherently high variability of this gas due to a marked daily cycle (Conrad et al., 1982; Table 2).

Measured mixing ratios of $CO_2$ were on average 2 ppm higher than those observed at ASC and had uncertainties in the same order of magnitude (Conway et al., 2012; Table 2). This offset was rather constant during the two cruises, being consistent with the observed trend at ASC between May and July when only slight changes were reported. Although no obvious system failures were detected on the NDIR analyzer or the measurement setup itself, this is not yet an automated system and because of the manual operation higher or lower flushing times may have occurred. On the other hand, the comparatively high scatter obtained could have been due to the fact that

**Combined underway measurements of $N_2O$, CO and $CO_2$**

D. L. Arévalo-Martínez et al.

the measuring interval was too short, generating only a few data points to produce the mean value for each measurement period. Additionally, is seems also likely that some remaining air from the equilibrator circuit could have affected the results due to the insufficient flushing of the gas lines after switching between atmospheric and oceanic measurements. Nearly 50 % of the $CO_2$ gas mixing ratios measured with our system were within the uncertainty of the monthly mean value recorded at ASC (387.7–391.5 ppm) which does not exclude, however, some problem with the sample handling at the control unit. Longer flushing times and/or increased pumping speed should be tested in further at-sea deployments in order to improve underway $CO_2$ atmospheric measurements.

The two-month record of highly resolved surface water measurements was used to trace the development of the seasonal equatorial upwelling in the eastern equatorial Atlantic Ocean. Such seasonality is mainly controlled by the strength and variability of trade winds and the meridional displacement of the Intertropical Convergence Zone (ITCZ, Philander and Pacanowski, 1986; Grodsky et al., 2008): a warm period occurs between March and May when the ITCZ is displaced northward. This period is characterized by low wind speeds, reduced vertical transport and the highest surface temperatures. An active upwelling season, which proceeds with increasing intensity between June and August emerges as a response to enhanced trade wind speeds, shoaling of the pycnocline and increased vertical advection of cold, nutrient-rich waters to the surface. Subsequent weakening of the winds towards September–October reduces the turbulence and the stratified condition of the system starts to be restored reaching the maximal temperatures on March (Vinogradov, 1981). Figure 10 shows the computed $C_{N_2O}$ and $fCO_2$ from two equatorial sections before (EQ I, Fig. 6) and after (EQ II, Fig. 6) the onset of the equatorial upwelling (SST change from 27.16 °C on 8 June to 23.40 °C on 13 June). Evaluation of these sections for $N_2O$ evidenced the presence of supersaturated waters with saturation levels up to 148 % (mean: $121 \pm 7$ %). Moreover, a strong correlation between $C_{N_2O}$ values and SST was observed ($r^2 = 0.99$), providing further indication that surface $N_2O$ supersaturation was in fact produced as

**Combined underway measurements of N₂O, CO and CO₂**

D. L. Arévalo-Martínez et al.

Title Page

Abstract | Introduction

Conclusions | References

Tables | Figures

|◄ | ►|

◄ | ►

Back | Close

Full Screen / Esc

Printer-friendly Version

Interactive Discussion

a result of the upwelling of $N_2O$-enriched waters. A similar strong correlation was found by Walter et al. (2004) in the equatorial band between 0–2° N and 23.5–26° W where it was also employed as an indicator of upwelling. Surface distribution of $N_2O$ increased from May to June in response to advection of cold supersaturated waters from the equatorial upwelling and higher $C_{N_2O}$ values were found east of 12° W on both equatorial sections. The mean $C_{N_2O}$ values for the first and second equatorial sections were $7.01 \pm 0.17\,\mathrm{nmol\,L^{-1}}$ and $8.14 \pm 0.87\,\mathrm{nmol\,L^{-1}}$ respectively, indicating a 16 % enhancement for the latter. This is consistent with the observation that surface distribution of $N_2O$ in the open ocean is predominantly driven by physical forcing (Nevison et al., 1995). Comparison of the two equatorial sections for $f\mathrm{CO_2}$ showed increasing values from middle May to early June in association to lower temperatures as a consequence of the equatorial upwelling, and the highest values were found in the eastern side of the area covered by the cruise track, particularly in the vicinity of 12 to 10° W (Fig. 10). These results are consistent with observations reported by previous studies in the eastern tropical Atlantic Ocean (Andrié et al., 1986; Bakker et al., 1999; Lefèvre et al., 2008). A strong enhancement in surface $f\mathrm{CO_2}$ was observed during the second equatorial section (lower right panel on Fig. 10), coinciding with the temporal progression and the spatial location of the more intense upwelling area (Grodsky et al., 2008).

Seawater CO concentrations during MSM 18-2 were highly variable ranging from 0.12 to $1.1\,\mathrm{nmol\,L^{-1}}$ (mean $0.37 \pm 0.19\,\mathrm{nmol\,L^{-1}}$) with saturation ratios up to 17.21 (mean $5.97 \pm 3.10$), indicating persistent supersaturation conditions over the time spanned for the cruise. These values are well within the ranges reported for surface waters by Stubbins et al. (2006) during a south-north transect on the Atlantic Ocean ($0.2$–$2.6\,\mathrm{nmol\,L^{-1}}$) and by Kitidis et al. (2011) on the Mauritanian upwelling ($0.4$–$6.2\,\mathrm{nmol\,L^{-1}}$). Similar seawater CO concentrations ($0.40$–$2.4\,\mathrm{nmol\,L^{-1}}$) were also reported for the western equatorial Pacific by Bates et al. (1993) and Mastueda et al. (2000). However, most of our values lie within the lower range of the measurements by previous studies suggesting regional dissimilarities that might be attributed to differences in chromophoric dissolved organic matter (CDOM) absorbance, wind

speed, nutrient and chlorophyll distributions as well as a distinct oceanographic setup (Conrad et al., 1982; Day and Faloona, 2009; Kitidis et al., 2011).

A strong diel cycle was observed in CO concentrations with maximum values in the afternoon (mean $0.65 \pm 0.19\,\mathrm{nmol\,L^{-1}}$) and minimum values in the early morning (mean $0.20 \pm 0.08\,\mathrm{nmol\,L^{-1}}$). An example of this daily pattern is shown in Fig. 11, where CO concentrations during a west to east equatorial section between 21° W and 10° W (EQ II, Fig. 6) are displayed. Since this is a narrow band with rather uniform meteorological conditions the observed changes in CO seemed to be mostly driven by the daily cycle of solar radiation. In accordance with previous studies (Conrad et al., 1982; Stubbins et al., 2006) a delay of 2–4 h between the maximal diurnal light intensity (PAR) and the maximal CO concentration was observed, indicating a progressive release of CO after photochemical activation of the oxidative processes responsible for its formation from CDOM (Day and Faloona, 2009; Kitidis et al., 2011). In addition to light, a comprehensive analysis of the CO distribution should also include CDOM absorbance, wind speed and chlorophyll among others. However, such discussion is not addressed here since it's out of the scope of this paper.

## 5 Summary and conclusions

A new system for underway measurements of $N_2O$, CO and $CO_2$, which combines OA-ICOS and the well-established NDIR with a Weiss-type equilibrator has been developed and tested. The gas equilibration process in the chamber employed on this system occurs at a faster rate in comparison to other equilibrators of similar design, with a typical response time of 2.5 min for $N_2O$ and $CO_2$, and 45 min for CO. Longer equilibration times for CO are caused by its lower solubility, although the speed with which the sources and sinks change its concentrations in surface waters makes it possible to trace its daily variations with rather high resolution.

The DLT-100 analyzer has been shown to be highly stable with short optimal integration times, as well as to have lower detection limits when compared to instruments

using similar techniques (e.g. QCL). Furthermore, experimental results showed that the DLT-100 delivers data with precision that matches the suggested optimal precision to be achieved for highly-sensitive field measurements of N$_2$O. A two-week calibration interval of the DLT-100 has been shown to be sufficient to obtain highly accurate N$_2$O and CO data. However, operation of the system in areas of elevated surface gas concentrations might require more frequent calibrations in order to ensure the same accuracy as for the lower concentration range. The analyzer's response over time can be properly described by means of quadratic functions both in the lower and upper boundaries of its operational range for N$_2$O and CO, such that proper data corrections can be performed when the required calibration frequency cannot be achieved during field unattended deployment of the underway system.

Field performance of the N$_2$O/CO/CO$_2$ system was tested during two oceanographic campaigns on the equatorial Atlantic Ocean. Standard gas measurements of N$_2$O and CO were stable over a 64 day period with an overall instrument drift lower than 1 %. Accuracy loss for CO data was encountered during MSM 18-3, probably in association with steep temperature changes from which the analyzer did not completely recover because of its continuous use at temperatures close to the upper boundary of its operational range. Long-term deployment of the system for at-sea measurements would therefore require appropriate ventilation of the analyzer, in particular when operated in warm tropical environments. Comparison of $C_{N_2O}$ and $f$CO$_2$ data computed from measurements carried out by means of the underway system described here and discrete, well-established methods showed good agreement during both cruises with deviations most likely due to a temporal mismatch when crossing through sharp gradients. Furthermore, the functioning of the NDIR analyzer while coupled into the N$_2$O/CO/CO$_2$ system was tested by direct comparison with the autonomous GO system. Results showed a remarkable agreement between setups, suggesting a reliable operation of our underway analytical system.

Results from atmospheric measurements agree reasonably well with monthly means of the NOAA atmospheric sampling location at Ascension Island, although further tech-

nical improvements are required in order to improve the obtained accuracy. A two-month record of $N_2O$ and $CO_2$ was used to trace the development of the equatorial upwelling in the Atlantic Ocean, providing the first high resolution view of the temporal and spatial surface distribution patterns of these two climate-relevant gases on the area. Moreover, concentrations of dissolved $N_2O$, CO and $CO_2$ during the MSM 18-2 cruise were in good agreement with previous studies in different oceanic areas. These results put forward the potential of the underway method employed as a tool to unravel fine scale biological and physical processes on the surface ocean which might be otherwise ignored due to lack of resolution.

In conclusion, this new setup used to perform simultaneous underway $N_2O$, CO and $CO_2$ measurements has been shown to have good short and long-term stability, accuracy and improved precision in comparison with systems based upon similar infrared techniques and traditional discrete methods. The relatively simple setup performed well during its first major field deployment on the equatorial Atlantic Ocean thus suggesting its potential to be used continuously not only onboard research vessels but also on voluntary observing ships (VOS).

Title Page

Abstract | Introduction

Conclusions | References

Tables | Figures

◄ | ►

◄ | ►

Back | Close

Full Screen / Esc

Printer-friendly Version

Interactive Discussion

# References

Allan, D. W.: Statistics of atomic frequency standards, Proc. IEEE, 54, 221–230, 1966.

Andrié, C., Oudot, C., Genthon, C, and Merlivat, L.: $CO_2$ fluxes in the tropical Atlantic during FOCAL cruises, J. Geophys. Res., 21, 11741–11755, 1986.

5   Baer, D. S., Paul, J. B., Gupta, M., and O'keefe, A.: Sensitive absorption measurements in the near-infrared region using off-axis integrated-cavity output spectroscopy, Appl. Phys. B, 75, 261–265, 2002.

Bakker, D. C. E., de Baar, H. J. W., and de Jong, E.: Dissolved carbon dioxide in tropical east Atlantic surface waters, Phys. Chem. Earth B, 24, 399–404, 1999.

10  Bange, H. W., Rapsomanikis, S., and Andreae, M. O.: Nitrous oxide in coastal waters, Global Biogeochem. Cy., 10, 197–207, 1996a.

Bange, H. W., Rapsomanikis, S., and Andreae, M. O.: The Aegean Sea as a source of atmospheric nitrous oxide and methane, Mar. Chem., 53, 41–49, 1996b.

Bates, T. S., Kelly, K. C., and Johnson, J. E.: Concentrations and fluxes of dissolved biogenic
15  gases (DMS, $CH_4$, CO, $CO_2$) in the equatorial Pacific during the SAGA 3 experiment, J. Geophys. Res., 98, 16969–16977, 1993.

Bates, T. S., Kelly, K. C., Johnson, J. E., and Gammon, R. H.: Regional and seasonal variations in the flux of oceanic carbon monoxide to the atmosphere, J. Geophys. Res., 100, 23093–23101, 1995.

20  Becker, M., Andersen, N., Fiedler, B., Fietzek, P., Körtzinger, A., Steinhoff, T., and Friedrichs, G.: Using cavity ringdown spectroscopy for continuous monitoring of $\delta^{13}C(CO_2)$ and $fCO_2$ in the surface ocean, Limnol. Oceanogr., 10, 752–766, 2012.

Burch, D. E., Singleton, E. B., and Williams, D.: Absorption line broadening in the infrared, Appl. Optics, 1, 359–363, 1962.

25  Butler, J. H., Elkins, J. W., Brunson, C. H., Egan, K. B., Thompson, T. M., Conway, T. J., and Hall, B. D.: Trace gases in and over the West Pacific and East Indian Oceans during the El Niño-Southern Oscillation event of 1987, Data Rep. ERL ARL-16, Air Resour. Lab., Natl. Oceanic and Atmos. Admin., Silver Spring, Maryland, 104 pp., 1988.

Conrad, R., Seiler, W., Bunse, G., and Giehl, H.: Carbon monoxide in seawater (Atlantic
30  Ocean), J. Geophys. Res., 87, 8839–8852, 1982.

Conway, T. J., Lang, P. M., and Masarie, K. A.: Atmospheric carbon dioxide dry air mole fractions from the NOAA ESRL Carbon Cycle Cooperative Global Air Sampling Network, 1968–

Title Page

Abstract | Introduction

Conclusions | References

Tables | Figures

◄◄ | ►►

◄ | ►

Back | Close

Full Screen / Esc

Printer-friendly Version

Interactive Discussion

2011, available at: ftp://ftp.cmdl.noaa.gov/ccg/co2/flask/event/ (last access: 15 August 2012), 2012.

Day, D. A. and Faloona, I.: Carbon monoxide and chromophoric dissolved organic matter cycles in the shelf waters of the northern California upwelling system, J. Geophys. Res., 114, C01006, doi:10.1029/2007JC004590, 2009.

Denman, K. L., Brasseur, G., Chidthaisong, A., Ciais, P., Cox, P. M., Dickinson, R. E., Hauglustaine, D., Heinze, C., Holland, E., Jacob, D., Lohmann, U., Ramachandran, S., da Silva Dias, P. L., Wofsky, S. C., and Zhang, X.: Couplings between changes in the climate system and biogeochemistry, in: Climate Change 2007: The Physical Science Basis, Contribution of Working Group I to the Fourth Assessment Report of the Intergovernmental Panel on Climate Change, edited by: Solomon, S., Qin, D., Manning, M., Chen, Z., Marquis, M., Averyt, K. B., Tignor, M., and Miller, H. L., Cambridge University Press, Cambridge, UK and New York, NY, USA, 499–587, 2007.

Dickson, A. G., Sabine, C. L., and Christian, J. R. (Eds.): Guide to best practices for ocean $CO_2$ measurements, PICES Special Publication 3, 191 pp., 2007.

Dlugokencky, E. J., Lang, P. M., and Masarie, K. A.: Atmospheric $N_2O$ dry air mole fractions from the NOAA GMD Carbon Cycle Cooperative Global Air Sampling Network, 1997–2010, version: 9 November 2011, 2011.

Dyroff, C.: Optimum signal-to-noise ratio in off-axis integrated cavity output spectroscopy, Opt. Lett., 36, 1110–1112, 2011.

Forster, P., Ramaswamy, V., Artaxo, P., Bernsten, T., Betts, R., Fahey, D. W., Haywood, J., Lean, J., Lowe, D. C., Myhre, G., Nganga, J., Prinn, R., Raga, G., Schulz, M., and Van Dorland, R.: Changes in atmospheric constituents and in radiative forcing, in: Climate Change 2007: The Physical Science Basis, Contribution of Working Group I to the Fourth Assessment Report of the Intergovernmental Panel on Climate Change, edited by: Solomon, S., Qin, D., Manning, M., Chen, Z., Marquis, M., Averyt, K. B., Tignor, M., and Miller, H. L., Cambridge University Press, Cambridge, UK and New York, NY, USA, 129–234, 2007.

Friedrichs, G.: Sensitive absorption methods for quantitative gas phase kinetic measurements, Part 2: Cavity ringdown spectroscopy, Z. Phys. Chem., 222, 31–61, 2008.

Grodsky, S. A., Carton, J. A., and McClain, C. R.: Variability of upwelling and chlorophyll in the equatorial Atlantic, Geophys. Res. Lett., 35, L03610, doi:10.1029/2007GL032466, 2008.

Gülzow, W., Rehder, G., Schneider, B., Schneider, J., Deimling, V., and Sadkowiak, B.: A new method for continuous measurement of methane and carbon dioxide in surface waters us-

ing off-axis integrated cavity output spectroscopy (ICOS): an example from the Baltic Sea, Limnol. Oceanogr.: Methods, 9, 176–184, 2011.

Hendriks, D. M. D., Dolman, A. J., van der Molen, M. K., and van Huissteden, J.: A compact and stable eddy covariance set-up for methane measurements using off-axis integrated cavity output spectroscopy, Atmos. Chem. Phys., 8, 431–443, doi:10.5194/acp-8-431-2008, 2008.

Herriott, D., Kogelnik, H., and Kompfner, R.: Off-axis paths in spherical mirror interferometers, Appl. Optics, 3, 523–526, 1964.

Hupp, J.: The importance of water vapor measurements and corrections, Application note # 129 v. March 2010, LI-COR Biosciences Inc., 8 pp., 2011.

Johnson, J. E.: Evaluation of a seawater equilibrator for shipboard analysis of dissolved oceanic trace gases, Anal. Chim. Acta, 395, 119–132, 1999.

Johnson, K., Willis, K., Butler, D., Johnson, W., and Wong, C.: Coulometric total carbon dioxide analysis for marine studies: maximizing the performance of an automated gas extraction system and coulometric detector, Mar. Chem., 44, 167–187, 1993.

Kasyutich, V. L., Bale, C. S. E., Canosa-Mas, C. E., Perang, C., Vaughan, S., and Wayne, R. P.: Cavity-enhanced absorption: detection of nitrogen dioxide and iodine monoxide using a violet laser diode, Appl. Phys. B, 76, 691–697, 2003.

Kitidis, V., Tilstone, G. H., Smyth, T. J., Torres, R., and Law, C. S.: Carbon monoxide emission from a Mauritanian upwelling filament, Mar. Chem., 127, 123–133, 2011.

Körtzinger, A., Thomas, H., Schneider, B., Gronau, N., Mintrop, L., and Duinker, J. C.: At sea intercomparison of two newly designed underway $pCO_2$ systems – encouraging results, Mar. Chem., 52, 133–145, 1996.

Körtzinger, A., Mintrop, L., Wallace, D. W. R., Johnson, K. M., Neil, C., Tilbrook, B., Towler, P., Inoue, H. Y., Ishii, M., Shaffer, G., Torres Saavedra, R. F., Ohtaki, E., Yamashita, E., Poisson, A., Brunet, C., Schauer, B., Goyet, C., and Eischeid, G.: The international at-sea intercomparison of $fCO_2$ systems during the R/V *Meteor Cruise* 36/1 in the North Atlantic Ocean, Mar. Chem., 72, 171–192, 2000.

Kroon, P. S., Hensen, A., Jonker, H. J. J., Zahniser, M. S., van't Veen, W. H., and Vermeulen, A. T.: Suitability of quantum cascade laser spectroscopy for $CH_4$ and $N_2O$ eddy covariance flux measurements, Biogeosciences, 4, 715–728, doi:10.5194/bg-4-715-2007, 2007.

Title Page

Abstract | Introduction

Conclusions | References

Tables | Figures

◄ | ►►|

◄ | ►

Back | Close

Full Screen / Esc

Printer-friendly Version

Interactive Discussion

Lefèvre, N., Guillot., A., Beaumont, L., and Danguy, T.: Variability of $f$CO$_2$ in the eastern tropical Atlantic from a moored buoy, J. Geophys. Res., 113, C01015, doi:10.1029/2007JC004146, 2008.

Lewis, E. and Wallace, D. W. R.: Program developed for CO$_2$ system calculations. ORNL/CDIAC-105, Carbon Dioxide Information and Analysis Center, Oak Ridge National Laboratory, US Department of energy, Oak Ridge, 1998.

LI-COR: LI-6252 CO$_2$ analyzer operating and service manual, LI-COR Biosciences Inc., Publication No. 9003–60, Lincoln, Nebraska, USA, 121 pp., 1996.

Maddaloni, P., Gagliardi, G., Malara, P., and De Natale, P.: Off-axis integrated-cavity-output spectroscopy for trace-gas concentration measurements: modeling and performance, J. Opt. Soc. Am. B, 23, 1938–1945, 2006.

Matsueda, H., Inque, H. Y., Asanuma, I., Aoyama, M., and Ishii, M.: Carbon monoxide and methane in surface seawater of the tropical Pacific Ocean, in: Dynamics and Characterization of Marine Organic Matter, edited by: Handa, N., Tanoue, E., and Hama, T., Terrapup/Kluwer, Japan, 485–508, 2000.

Mazurenka, M., Orr-Ewing, A. J., Perevall, R., and Ritchie, G. A. D.: Cavity ringdown and cavity enhanced spectroscopy using diode lasers, Annu. Rep. Prog. Chem. C, 101, 100–142, 2005.

McDermitt, D. K., Welles, J. M., and Eckles, R. D.: Effects of temperature, pressure and water vapor on gas phase infrared absorption by CO$_2$, LI-COR Biosciences, Inc., 5 pp., 1993.

Mintrop, L., Pérez, F. F., Gonlález-Dávila, M., Santana-Casiano, J. M., and Körtzinger, A.: Alkalinity determination by potentiometry: intercalibration using three different methods, Cienc. Mar., 26, 23–37, 2000.

Mojica-Prieto, F. J. and Millero, F. J.: The values of pK1 + pK2 for the dissociation of carbonic acid in seawater, Geochim. Cosmochim. Ac., 66, 2529–2540, 2002.

Nelson, D. D., McManus, B., Urbanski, S., Herndon, S., and Zahniser, M. S.: High precision measurements of nitrous oxide and methane using thermoelectrically cooled mid-infrared quantum cascade lasers and detectors, Spectrochim. Acta A., 60, 3325–3335, 2004.

Nevison, C. D., Weiss, R. F., and Erikson III, D. J.: Global oceanic emissions of nitrous oxide, J. Geophys. Res., 100, 15809–15820, 1995.

Novelli, P. C. and Masarie, K. A.: Atmospheric carbon monoxide dry air mole fractions from the NOAA ESRL Carbon Cycle Cooperative Global Air Sampling Network, 1988–2011, available at: ftp://ftp.cmdl.noaa.gov/ccg/co/flask/event/(last access: 18 September 2012), 2012.

Title Page

Abstract | Introduction

Conclusions | References

Tables | Figures

◄ | ►

◄ | ►

Back | Close

Full Screen / Esc

Printer-friendly Version

Interactive Discussion

O'Keefe, A. and Deacon, D. A. G.: Cavity ring-down optical spectrometer for absorption measurements using pulsed laser sources, Rev. Sci. Instrum., 59, 2544–2551, 1988.

Paul, J. B., Lapson, L., and Anderson, J. G.: Ultrasensitive absorption spectroscopy with a high-finesse optical cavity and off-axis alignment, Appl. Optics, 40, 4904–4910, 2001.

Philander, S. G. H. and Pacanowski, R. C.: A model of the seasonal cycle in the Tropical Atlantic Ocean, J. Geophys. Res., 91, 14192–14206, 1986.

Pierrot, D., Neill, C., Sullivan, K., Castle, R., Wanninkhof, R., Lüger, H., Johannenssen, T., Olsen, A., Feely, R. A., and Cosca, C. E.: Recommendations for autonomous underway $pCO_2$ measuring systems and data-reduction routines, Deep-Sea Res. II, 56, 512–522, 2009.

Prather, M., Ehhalt, D., Dentener, F., Derwent, R., Dlugokencky, E., Holland, E., Isaksen, I., Katima, J., Kirchhoff, V., Matson, P., Midgley, P., and Wang, M.: Atmospheric chemistry and greenhouse gases, in: Climate Change 2001: The Physical Science Basis, Contribution of Working Group I to the Third Assessment Report of the Intergovernmental Panel on Climate Change, edited by: Houghton, J. T., Ding, Y., Griggs, D. J., Noguer, M., van der Linden, P. J., Dai, X., Maskell, K., and Johnson, C. A., Cambridge University Press, Cambridge, UK and New York, NY, USA, 239–287, 2001.

Stubbins, A., Uher, G., Kitidis, V., Law, C. S., Upstill-Goddard, R. C., and Woodward, E. M. S.: The open-ocean source of atmospheric carbon monoxide, Deep-Sea. Res. II, 53, 1685–1694, 2006.

Vinogradov, M.: Ecosystems of equatorial upwellings, in: Analysis of Marine Ecosystems, edited by: Longhurst, A. R., Academic Press, London, 69–93, 1981.

Walter, S., Bange, H. W., and Wallace, D. W. R.: Nitrous oxide in the surface layer of the tropical North Atlantic Ocean along a west to east transect, Geophys. Res. Lett., 31, L23S07, doi:10.1029/2004GL019937, 2004.

Walter, S., Bange, H. W., Breitenbach, U., and Wallace, D. W. R.: Nitrous oxide in the North Atlantic Ocean, Biogeosciences, 3, 607–619, doi:10.5194/bg-3-607-2006, 2006.

Weiss, R. F.: Carbon dioxide in water and seawater: the solubility of a non-ideal gas, Mar. Chem., 2, 203–215, 1974.

Weiss, R. F.: Determinations of carbon dioxide and methane by dual catalyst flame ionization chromatography and nitrous oxide by electron capture chromatography, J. Chromatogr. Sci., 19, 611–616, 1981.

Weiss, R. F. and Price, B. A.: Nitrous oxide solubility in water and seawater, Mar. Chem., 8, 347–359, 1980.

**Combined underway measurements of $N_2O$, CO and $CO_2$**

D. L. Arévalo-Martínez et al.

| | |
|---|---|
| Title Page | |
| Abstract | Introduction |
| Conclusions | References |
| Tables | Figures |
| ◄◄ | ►► |
| ◄ | ► |
| Back | Close |
| Full Screen / Esc | |
| Printer-friendly Version | |
| Interactive Discussion | |

Weiss, R. F., Van Woy, F. A., and Salameh, P. K.: Surface water and atmospheric carbon dioxide and nitrous oxide observations by shipboard automated gas chromatography: results from expeditions between 1977 and 1990, Scripps Instit. Oceanogr. Ref. 92–11, Scripps Institution of Ocenography, San Diego, USA, 1992.

5  Werle, P., Mücke, R., and Slemr, F.: The limits of signal averaging in atmospheric trace-gas monitoring by tunable diode-laser absorption spectroscopy (TDLAS), Appl. Phys. B, 57, 131–139, 1993.

Wiesenburg, D. A. and Guinasso Jr., N. L.: Equilibrium solubilities of methane, carbon monoxide, and hydrogen in water and sea water, J. Chem. Eng. Data, 24, 356–360, 1979.

10  Wilhelm, E., Battino, R., and Wilcock, R. J.: Low-pressure solubility of gases in liquid water, Chem. Rev., 77, 1977.

Zellweger, C., Steinbacher, M., and Buchmann, B.: Evaluation of new laser spectrometer techniques for in-situ carbon monoxide measurements, Atmos. Meas. Tech., 5, 2555–2567, doi:10.5194/amt-5-2555-2012, 2012.

**Combined underway measurements of N$_2$O, CO and CO$_2$**

D. L. Arévalo-Martínez et al.

Title Page

Abstract | Introduction

Conclusions | References

Tables | Figures

◄ | ►

◄ | ►

Back | Close

Full Screen / Esc

Printer-friendly Version

Interactive Discussion

**Table 1.** Results of the calibration experiment carried out over a 14 day period. The MD values (cf. Eq. 5) calculated from 3 min averages of measurements for each standard gas are presented.

| Date and time (UTC) | N$_2$O [ppb] | | | CO [ppb] | |
|---|---|---|---|---|---|
| | 322.5 | 362.3 | 746.0 | 233.5 | 255.5 |
| 21 Dec 2010 10:52:02 | 0.094 % | −0.0055 % | −0.70 % | 0.13 % | 1.08 % |
| 21 Dec 2010 15:34:07 | 0.050 % | 0.017 % | −0.80 % | 0.11 % | 1.11 % |
| 22 Dec 2010 12:58:07 | −0.20 % | −0.130 % | −0.97 % | 0.04 % | 0.77 % |
| 29 Dec 2010 13:50:36 | 0.047 % | 0.075 % | −0.85 % | 1.16 % | 1.35 % |
| 03 Jan 2011 10:11:32 | 0.057 % | 0.140 % | −0.81 % | 1.16 % | 1.78 % |

**Table 2.** Comparison of underway atmospheric measurements carried out during the MSM 18-2 and 18-3 cruises and monthly means from the NOAA sampling location at Ascension Island (7.96° S 14.4° W). All values expressed as mean ±SD.

| Time period | MSM 18-2/18-3 | | | ASC | | |
| --- | --- | --- | --- | --- | --- | --- |
| | $N_2O$ [ppb] | CO [ppb] | $CO_2$ [ppm] | $N_2O$ [ppb] | CO [ppb] | $CO_2$ [ppm] |
| May 2011 | | | | 323.86 ± 0.36 | 75.16 ± 12.75 | 389.10 ± 0.81 |
| | 322.64 ± 0.70 | 86.12 ± 14.45 | 392.21 ± 2.67 | | | |
| Jun 2011 | | | | 324.11 ± 0.41 | 76.32 ± 9.63 | 389.33 ± 0.44 |
| | 323.63 ± 0.99 | 106.07 ± 17.40 | 392.31 ± 2.09 | | | |
| Jul 2011 | | | | 324.29 ± 0.32 | 97.74 ± 15.93 | 390.48 ± 0.85 |
| Overall | 323.04 ± 0.96 | 92.92 ± 18.19 | 392.26 ± 2.43 | 324.09 ± 0.40 | 83.20 ± 16.60 | 389.64 ± 0.94 |
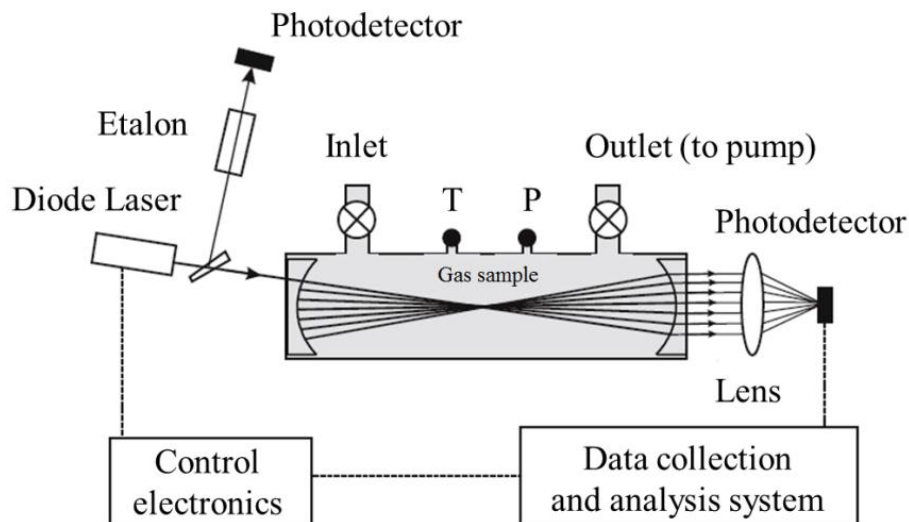
**Fig. 1.** Schematic diagram of an instrument based upon OA-ICOS (after Baer et al., 2002). The gas sample is conducted continuously through the cavity while the laser beam bounces multiple times between the highly-reflective (∼ 99.99 %) mirrors. "T" and "P" represent the cell's temperature and pressure sensors, respectively.
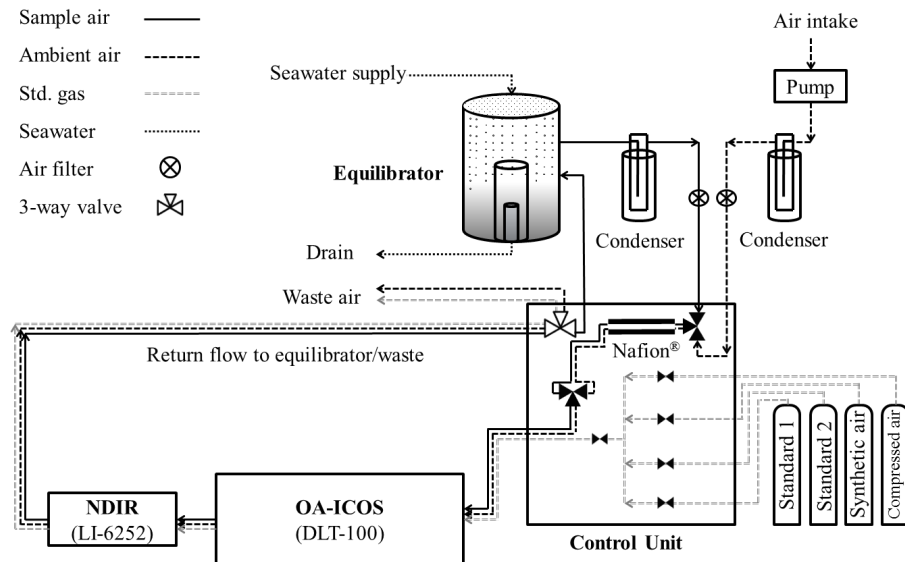
**Fig. 2.** Schematic drawing of the analytical system used for underway N$_2$O, CO and CO$_2$ measurements. Arrows indicate the direction of the gas/water flows.
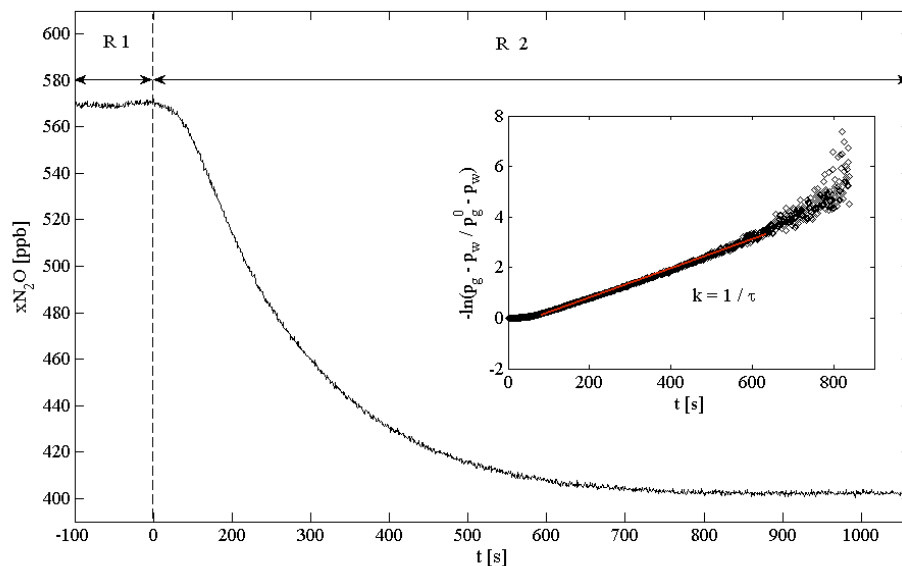
**Fig. 3.** Results of the step experiment carried out to determine the response time of the equilibrator. Water from the high concentration reservoir (R 1) was conducted through the equilibrator until stable readings were obtained and at $t = 0$, the flow was switched to the ambient air reservoir (R 2). A plot of the linearized change in $N_2O$ concentration over time was used to calculate the time constant $\tau$. The red line depicts the regression line to the data.
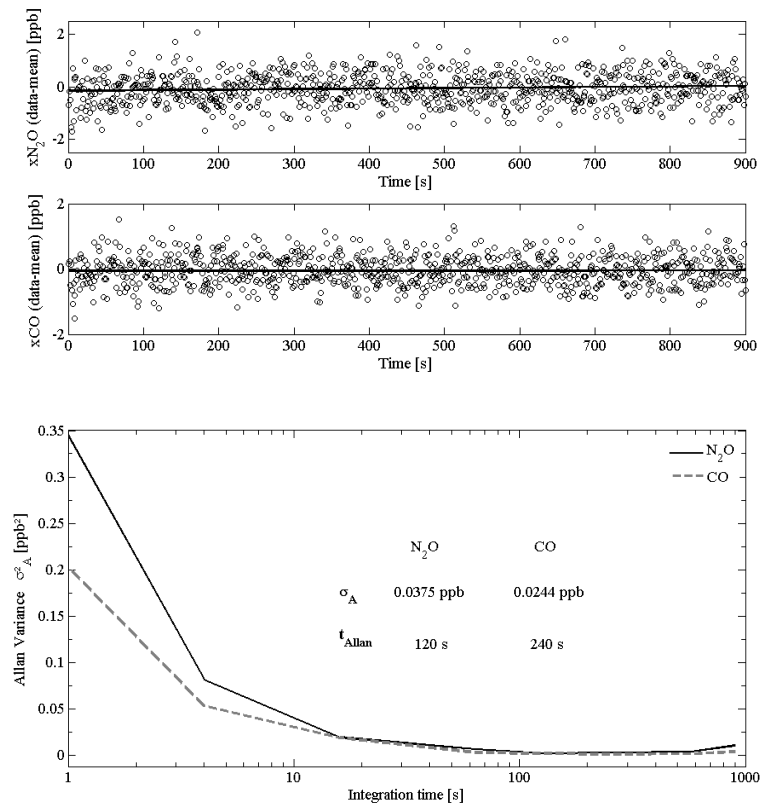
**Fig. 4.** Instrument drift test of the DLT-100 analyzer. Upper panel shows a time series of molar fractions of N$_2$O and CO over a 15 min period at a rate of 1 Hz. The results are presented as single data point deviation from the mean value and the corresponding linear regression lines are depicted. The Allan variance plot for N$_2$O and CO over the measurement period is shown in the lower panel, including the values of Allan standard deviation ($\sigma_A$) and optimal averaging times ($t_{Allan}$) at the minimum $\sigma_A^2$.
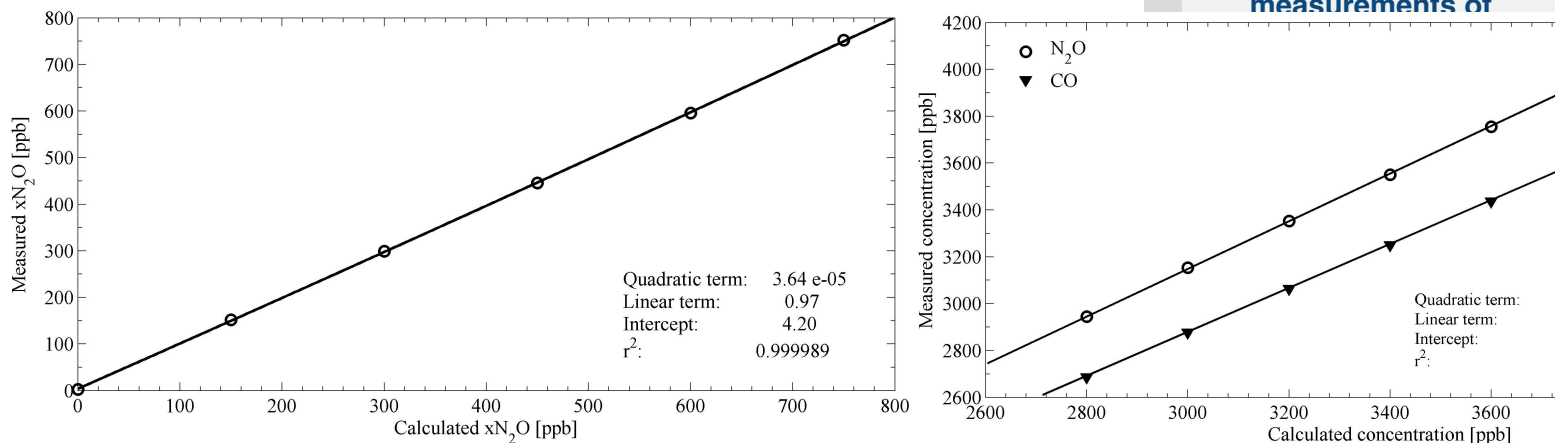
**Fig. 5.** Plots of the linearity tests performed on the DLT-100 analyzer. Regression lines of the corresponding quadratic fits applied are depicted. The upper panel shows a linearity plot for $N_2O$ on the concentration range from 0 to 750 ppb and the lower panel the corresponding plot for $N_2O$ and CO on the concentration range between 2800 and 4000 ppb.
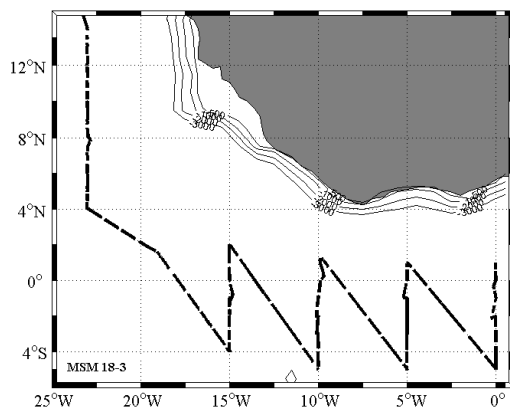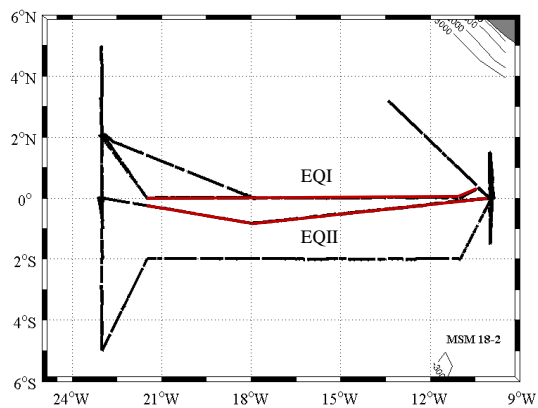
**Fig. 6.** Cruise tracks of the R/V *Merian* MSM 18-2 and 18-3 cruises. The red lines indicate two equatorial sections carried out before (EQI) and after (EQII) the onset of the equatorial upwelling (see Sect. 4 and Fig. 11).
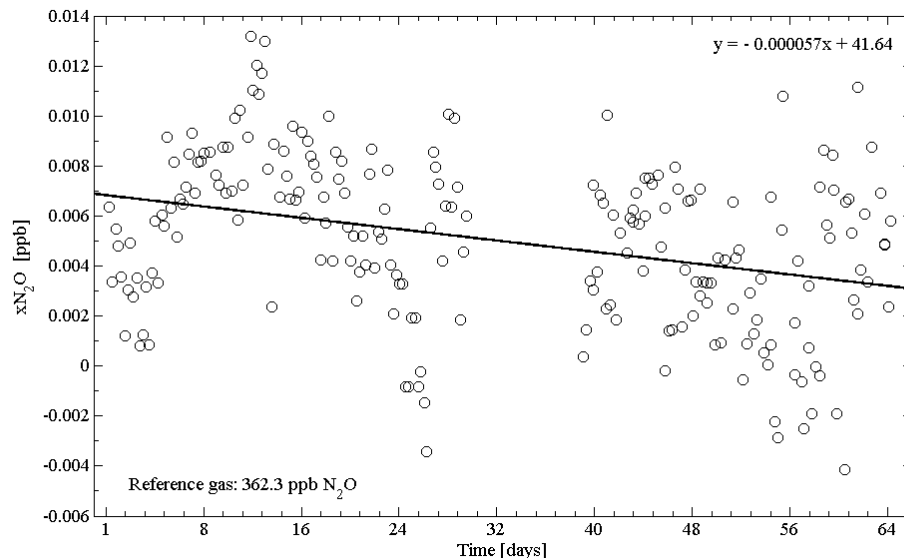
**Fig. 7.** $N_2O$ standard gas measurements carried out during the MSM 18-2 and 18-3 cruises between May–July 2011. Data are presented as the deviation of every single measurement period (3 min means) from the reference value (cf. Eq. 5). A linear regression to the data and the corresponding equation are also shown.

Title Page

Abstract | Introduction

Conclusions | References

Tables | Figures

◄ | ►

◄ | ►

Back | Close

Full Screen / Esc

Printer-friendly Version

Interactive Discussion
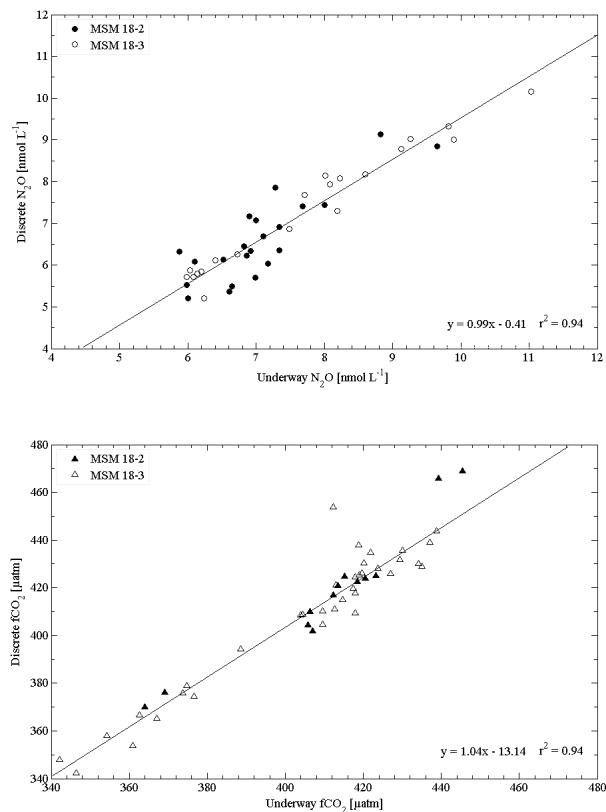
**Fig. 8.** Comparison of discrete and underway N$_2$O (top) and CO$_2$ (bottom) measurements during the MSM 18-2 and 18-3 cruises. A GC/ECD method was used for discrete N$_2$O samples whereas $f$CO$_2$ was calculated from discrete DIC and $T_A$ data. Regression lines are included on each plot.
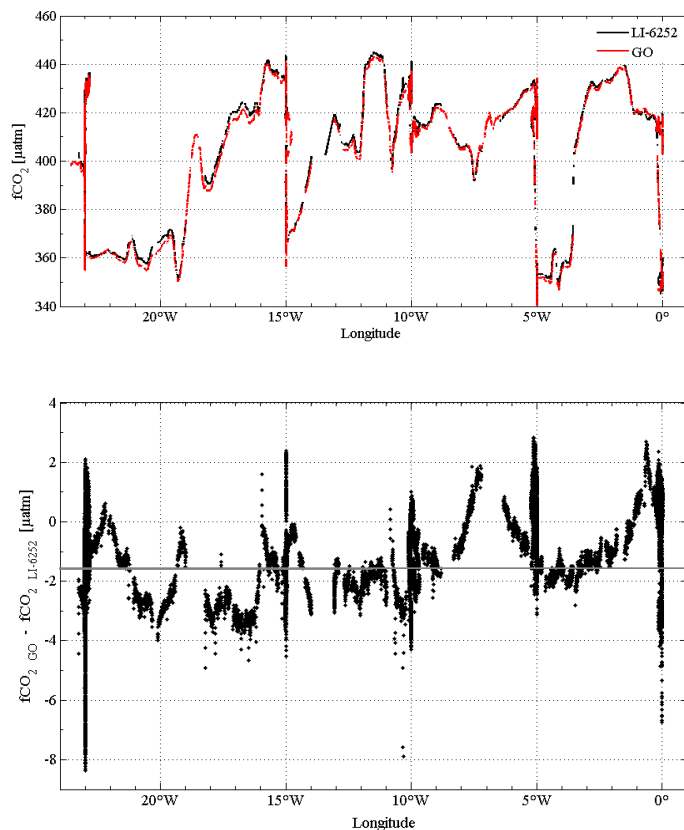
**Fig. 9.** Assessment of the LI-6252 performance during the MSM 18-3 cruise. A comparison of $f\mathrm{CO_2}$ computed from GO (red line) and LI-6252 (black line) data (top) as well as the $f\mathrm{CO_2}$ difference between both systems (bottom) is shown. The mean offset is represented by the grey line on the bottom panel.
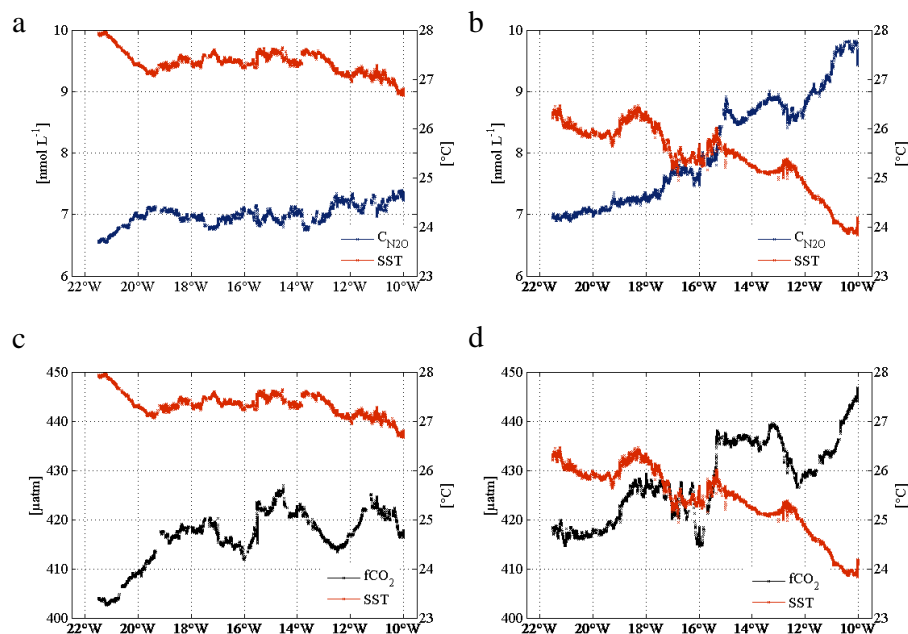
**Combined underway measurements of N₂O, CO and CO₂**

D. L. Arévalo-Martínez et al.

Title Page

Abstract | Introduction

Conclusions | References

Tables | Figures

◄ | ►

◄ | ►

Back | Close

Full Screen / Esc

Printer-friendly Version

Interactive Discussion

**Fig. 10.** Oceanic N$_2$O **(a, b)** and CO$_2$ **(c, d)** measured in two equatorial sections during the MSM 18-2 cruise (EQ I and EQ II, Fig. 6). The sections were done before (May, left) and after (June, right) the onset of the equatorial upwelling as indicated by the SST (in red).
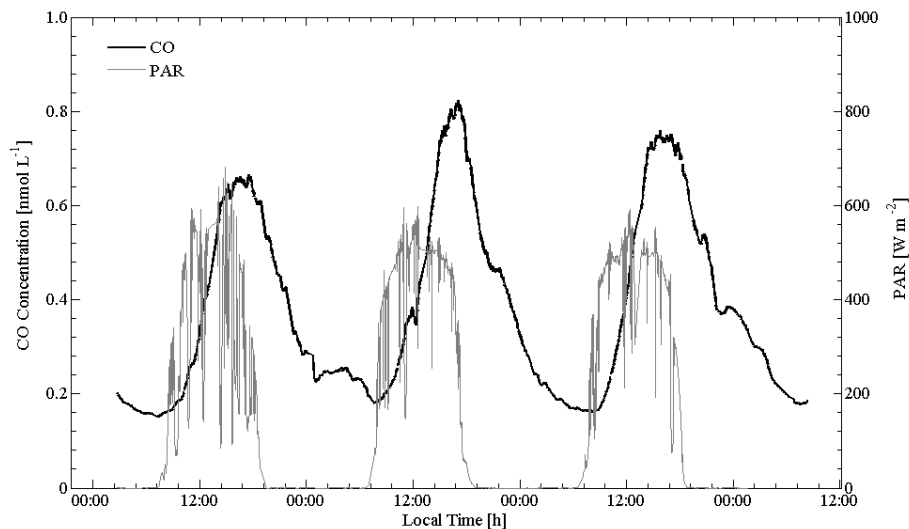
**Fig. 11.** CO concentration measured throughout an equatorial section (EQ II, Fig. 6) during the MSM 18-2 cruise. PAR = photosynthetically active radiation.